Integrative transcriptome analysis identified a BMP signaling pathway-regulated lncRNA AC068643.1 in IDH mutant and wild-type glioblastomas

GUO-HAO HUANG[1*], YU-CHUN PEI[1*], LIN YANG[1], KE-JIE MOU[2], JUN-HAI TANG[1], YAN XIANG[1], JUN LIU[1] and SHENG-QING LV[1]

[1]Department of Neurosurgery, Xinqiao Hospital, Third Military Medical University, Chongqing 400037; [2]Department of Neurosurgery, Bishan Hospital, Chongqing Medical University, Chongqing 402760, P.R. China

Received November 26, 2018; Accepted December 12, 2019

DOI: 10.3892/ol.2020.11542

Abstract. Glioblastomas (GBMs) are classified into isocitrate dehydrogenase (IDH) mutant (IDH^{MT}) and wild-type (IDH^{WT}) subtypes, and each is associated with distinct tumor behavior and prognosis. The present study aimed to investigate differentially expressed long non-coding (lnc)RNAs and mRNAs between IDH^{MT} and IDH^{WT} GBMs, as well as to explore the interaction and potential functions of these RNAs. A total of 132 GBM samples with RNA profiling data (10 IDH^{MT} and 122 IDH^{WT} cases) were obtained from The Cancer Genome Atlas, and 62/78 and 142/219 up/downregulated lncRNAs and mRNAs between IDH^{MT} and IDH^{WT} GBMs were identified, respectively. Multivariate Cox analysis of the dysregulated lncRNAs/mRNAs identified three-lncRNA and fifteen-mRNA signatures with independent prognostic value, indicating that these RNAs may serve roles in determining distinct tumor behaviors and prognosis of patients with $IDH^{MT/WT}$ GBMs. Functional analysis of the three lncRNAs revealed that they were primarily associated with cell stemness or differentiation. Pearson's correlation analysis revealed that the protective lncRNA AC068643.1 was significantly positively correlated with two key bone morphogenetic protein (BMP) signaling-associated mRNAs, Bone morphogenetic protein 2 (BMP2) and Myostatin (MSTN), from the 15 mRNAs. Further *in vitro* studies demonstrated that BMP2 and MSTN directly stimulated AC068643.1 expression. In conclusion, the present study identified a BMP signaling pathway-regulated lncRNA AC068643.1, which may contribute to the different tumor behaviors observed between IDH^{MT} and IDH^{WT} GBMs.

Correspondence to: Professor Sheng-Qing Lv or Professor Jun Liu, Department of Neurosurgery, Xinqiao Hospital, Third Military Medical University, 183 Xinqiao Street, Shapingba, Chongqing 400037, P.R. China
E-mail: lvsq0518@hotmail.com
E-mail: liujdoctor@163.com

*Contributed equally

Key words: IDH mutation, glioblastoma, lncRNA, prognostic, stemness

Introduction

Glioblastomas (GBMs) are the most common and deadliest tumors of the central nervous system (CNS) (1). According to multiple studies from different regions of the world, despite radical therapy involving maximal tumor resection and chemo/radiotherapy, the median survival time is only 14.6 months, and the 5-year survival rate is only 9.8% for patients with GBM (2-4). At present, the development of targeted molecular therapy for GBMs is unsatisfactory; therefore, investigation of GBM pathogenesis at the genetic and molecular levels is required.

Somatic mutations in isocitrate dehydrogenases (IDH) have been commonly identified in lower grade gliomas (LGG; WHO grade II and III) and secondary GBMs (5). Development of *IDH* mutant (IDH^{MT}) and *IDH* wild-type (IDH^{WT}) gliomas is driven by different oncogenic processes, thus these subtypes present distinct molecular and clinical features (6). IDH^{WT} GBM is more aggressive compared with IDH^{MT} GBM, and the median survival time of patients with IDH^{MT} GBM is 31 months, whereas that of patients with IDH^{WT} GBM is <15 months (4,5). IDH^{MT} GBM only constitutes a small proportion of total GBM cases (5), suggesting that research investigating the underlying mechanisms of the disease should focus on IDH^{WT} GBM. However, tumor behaviors are closely associated with the altered gene expression patterns (7), and thus it is necessary to compare the transcriptomes of IDH^{MT} and IDH^{WT} GBM tissues, which may provide more valuable information than comparing IDH^{WT} GBM and normal brain tissue transcriptomes.

Long noncoding RNAs (lncRNAs), which are >200 nucleotides long, have attracted attention due to their multiple gene regulation functions at the transcriptional, post-transcriptional and epigenetic levels (8). Previous studies have indicated that lncRNAs are predominantly expressed in the CNS (9,10) and are spatio-temporally regulated to serve functions in the CNS development (11). Therefore, dysregulation of lncRNA

expression may contribute to a number of CNS diseases, including brain injuries, neurodegenerative diseases (12) and GBM (13,14). For example, Han *et al* (15) identified 1,308 lncRNAs dysregulated in GBM tissues compared with the normal brain tissues. LncRNAs serve a number of roles in GBM, including the involvement in the NEAT-1-regulated EGFR pathway (16), Hox transcript antisense intergenic RNA HOTAIR-regulated GBM proliferation (17,18) and stem-related lncRNA HIF1A-AS2-regulated GBM stemness maintenance (19). The present study aimed to identify differentially expressed lncRNAs (DE-lncRNAs) and mRNAs (DE-mRNAs) between IDH^{MT} and IDH^{WT} GBM by mining RNA sequencing data from The Cancer Genome Atlas database (TCGA), exploring their interactions and potential functions in mediating the different tumor behaviors observed in IDH^{MT} and IDH^{WT} GBM.

Materials and methods

GBM datasets and clinical samples. The present study was approved by The Medical Ethics Committee of The Second Affiliated Hospital (Xinqiao Hospital) of the Third Military Medical University, and written informed content was obtained from the patients. mRNA and lncRNA expression data and corresponding clinical information, including patient sex, age at diagnosis and Karnofsky Performance Status (KPS), for 132 GBM samples (122 IDH^{WT} and 10 IDH^{MT} cases) were obtained from TCGA database (cancer.gov/tcga). The datasets contained 19,676 protein-coding mRNAs and 9,599 lncRNAs. A total of 128 GBM samples (107 IDH^{WT} cases and 21 IDH^{MT} cases) with mRNA microarray data and corresponding clinical information were obtained from the Chinese Glioma Genome Atlas (CGGA; cgga.org.cn/download.jsp) database for further validation. In addition, 45 GBM samples (37 IDH^{WT} and 8 IDH^{MT} cases) and 12 normal peritumor tissues were obtained from patients in Xinqiao Hospital (Chongqing, China) for validating the bioinformatics analysis results (XQ cohort). The age of patients from XQ cohort ranged from 22 to 76 years old and the median age was 52.3 years old and the patients' male: female sex ratio was 1.67. The tumor and peritumor tissues were collected at the time of surgery and then immediately stored at -80˚C until use. Patients' clinicopathological characteristics are detailed in Table SI.

Cell culture and subcellular RNA extraction. SNB19 (authenticated by STR profiling) and SF295 (20) human GBM cell lines with <5 total passage times were obtained from the National Cancer Institute-60 (NCI-60) Cancer Cell Line Panel (dtp.cancer.gov/discovery_development/nci-60/default.htm), whereas LN229 and T98G glioma cells were obtained from ATCC. All cell lines were cultured as previously described (21). The total RNA was extracted using TRIzol® reagent (Invitrogen; Thermo Fisher Scientific Inc.), and subcellular RNA was extracted using RNA Subcellular Isolation kit (Active Motif, Inc.) according to the manufacturer's protocol.

Bone morphogenetic protein 2 (BMP2) and Myostatin (MSTN) cytokine treatment of T98G cells. T98G glioma cells were cultured in Minimum Essential Medium (Gibco; Thermo Fisher Scientific, Inc.) supplemented with 10% FBS (Gibco; Thermo Fisher Scientific, Inc.) at 37˚C in a humified 5% CO_2 atmosphere. Recombinant human BMP2 and MSTN (PeproTech, Inc.) cytokines were added to the T98G glioma cell line culture medium to achieve 10 and 50 ng/ml, respectively. The BMP2/MSTN medium was used for 4-5 days to culture T98G cells prior to harvesting the cells for the subsequent experiments.

Reverse transcription-quantitative (RT-q)PCR. Total RNA in cells or tissues was extracted by TRIzol® reagent (Invitrogen; Thermo Fisher Scientific Inc.) to perform (RT-q)PCR. For tissue RNA extraction, 50-100 mg tissues were added into 1 ml TRIzol® reagent and homogenized using Precellys 24 (Bertin Technologies). Then, 0.2 ml chloroform was added into the homogenized tissue-TRIzol mixture and incubated for 2-3 min and centrifuged at 12,000 g at 4˚*C* for 15 min for phase separation. After that, the RNA-contained upper aqueous phase was transferred to a new RNase/DNase-free Tube and 500 μl isopropanol was added to precipitate the RNA. After centrifugation at 12,000 g at 4˚C for 10 min, the supernatant was discarded and 1 ml 75% ethanol was added to wash the RNA. Finally, after the RNA pellet was air dried for 5-10 min, 20 μl RNase-free water was added to dissolve RNA pellet.

RNA reverse transcription was performed using a PrimeScript™ RT Master mix (Takara Bio, Inc.). The reaction condition was reverse transcript at 37˚C for 30 min and inactivation of reverse transcriptase at 85˚C for 5s. First-strand cDNA was detected using a Bio-Rad CFX96™ Real Time system using the iTaq™ universal SYBR® Green Supermix (both Bio-Rad Laboratories, Inc.) according to the manufacturer's protocol. The PCR conditions were as follows: 40 cycles of degeneration at 95˚C for 5 sec, and annealing and extension at 60˚C for 30 sec. mRNA relative expression levels were analyzed using the $2^{-\Delta\Delta Cq}$ method (22), and GAPDH was used as a housekeeping gene for baseline expression. For absolute qPCR, lncRNA AC068643.1 qPCR product was retrieved using an AxyPrep DNA Gel Extraction kit (Axygen; Corning, Inc.) to establish a standard curve. Small nucleolar RNA SNORA16A was used as an internal reference. Sequences of PCR primers were as follows: GAPDH forward, 5'-GACTCATGACCACAGTCCATGC-3' and reverse, 5'-AGAGGCAGGGATGATGTTCTG-3'; lncRNA AC068643.1 forward, 5'-GAAACTACAAGAAGATGCATCTGTCTT-3' and reverse, 5'-TATCTCTCTCTTGTGTTGCACCTTTTA-3'; BMP2 forward, 5'-CAGCTTCCACCATGAAGAATCTTTGG-3' and reverse, 5'-ATTCGGTGATGGAAACTGCTATTGTTT-3'; MSTN forward, 5'-GAAACAGCTCCTAACATCAGCAAAGAT-3' and reverse, 5'-AGACTCTGTAGGCATGGTAATGATTGT-3'; ATPase (ATP)13A5 forward, 5'-GAGTTTGGAAAGAAACTGGACTGGAAA-3' and reverse, 5'-GGCTTTCCCTTAGAAAAGATGAATGCT-3'; SNORA16A forward, 5'-CTTCCGCATAGCTGCTGTGGTCAA-3' and reverse, 5'-AGTTACAACAAACAGAACGGCGACC-3'.

Identification of DE-lncRNAs/mRNAs between IDH^{WT} and IDH^{MT} GBMs. GBM RNASeq HTSeq Level 3 (23) Agilent-based lncRNA/mRNA profiling datasets were obtained from TCGA database. DE-lncRNA/mRNAs (DERs) were identified using R 3.4.3 (24) software and the R/Bioconductor package 'edgeR' (version 3.20.6). The significant DERs were filtered based on $\log_2$ fold-change ≥2/≤-2 and $-\log_{10}$ adjusted P-value ≥2.

Survival analysis. Survival analysis was performed in the R studio (25) and R version 3.4.3 statistical environments. R package 'survival' was used to determine the prognostic DERs. For univariate Cox proportional hazards regression analysis, patient survival time, status (dead or alive) and lncRNA/mRNA expression levels were combined and processed using the 'coxph' function to explore the association between DERs and patient overall survival (OS). DERs with a hazard ratio (HR) value >1 were defined as risk RNAs, whereas those with HR <1 were defined as protective RNAs. DE-lncRNAs with P<0.001 and DE-mRNAs with P<0.01 were selected as survival-associated DERs. Similarly, for multivariate Cox regression analysis, the 'coxph' and 'step' functions from the R package 'survival' were used to determine the key lncRNAs/mRNAs associated with the survival of patients with GBM (survival-related DERs). Risk scores were established using the survival-related DERs, which were weighted using the regression coefficients in the multivariate Cox regression model, and a prognostic lncRNA/mRNA signature was constructed. Kaplan-Meier curves (using GraphPad Prism version 6.00 for Windows, graphpad.com/) were used to estimate the survival for patients between low/high-risk lncRNA/mRNA groups.

Integrative prediction analysis of lncRNA function. Pearson's correlation analysis was used to evaluate the co-expression relationship between prognostic lncRNAs and mRNAs. Correlation coefficient r>0.4 was considered as co-expressed, and co-expressed mRNAs were used to predict the function of lncRNAs using The Database for Annotation, Visualization and Integrated Discovery (david.ncifcrf.gov/). Functional enrichment results were limited to Gene Ontology (GO) terms, including biological process, cell components and molecular function, and Kyoto Encyclopedia of Genes and Genomes (KEGG) pathway categories. The presented results include the top 10 significantly enriched GO terms and top five enriched KEGG terms.

Statistical analysis. Data are presented as the mean ± standard deviation. Unpaired Students' t-test (two-tailed) was used to analyze the differences between the means of two groups. Pearson correlation analysis was used to establish the correlation between RNA expression levels. A Kruskal-Wallis test with Bonferroni's post-hoc correction was used for comparisons among multiple groups. P<0.05 was considered to indicate a statistically significant difference.

Results

Identification of prognostic DERs between IDH^{MT} and IDH^{WT} GBMs. To determine the key factors mediating different behaviors between IDH^{MT} and IDH^{WT} GBMs, DE-lncRNAs between the 122 IDH^{WT} and 10 IDH^{MT} GBM samples from TCGA database were investigated. Heatmap clustering analysis revealed that IDH^{WT} and IDH^{MT} GBMs presented distinct lncRNA expression patterns (Fig. 1A), demonstrating that IDH^{WT} and IDH^{MT} were distinct GBM subtypes. Using screening criteria $\log_2$ fold-change ≥1/≤-1 and -log10 adjusted P-value ≥2, 62 upregulated and 78 downregulated lncRNAs in IDH^{MT} GBMs were identified (Fig. 1B). To identify DE-lncRNAs that served roles in GBM, the DE-lncRNAs were subjected to an univariate Cox model. The results revealed that four lncRNAs were significantly associated with the patients' OS (P<0.001), among which AC068643.1 and AC022148.1 were protective lncRNAs (HR <1), whereas Linc01776 and Linc02036 were risk lncRNAs (HR >1) (Table SII). These OS-related lncRNAs were further subjected to a multivariate Cox model and the results revealed a three-lncRNA prognostic signature that best able to predict patients' survival. The three-lncRNA prognostic signature includes one protective lncRNA (AC068643.1) and two risk-associated lncRNAs (Linc01776 and Linc02036) (Table I; Fig. 1C). Using the three-lncRNA prognostic signature, a risk score was calculated for each patient with GBM. All patients were then divided into two groups: Low-risk (n=66) and high risk (n=66) using the median risk score as the cutoff value (Fig. 1C). Kaplan-Meier survival analysis revealed that the survival time of patients in the high-risk group was significantly shorter compared with the low-risk group [P=0.004, HR=1.779, 95% confidence interval (CI), 1.246-2.852; Fig. 1D]. Therefore, the lncRNA profile, COX and survival analyses identified three prognostic lncRNAs that may serve roles in determining the distinct properties of IDH^{WT} and IDH^{MT} GBM.

Previous studies have demonstrated that lncRNAs act through mRNA interaction (8,26); therefore, the present study sought to identify the target mRNAs that interacted with the three prognostic signature lncRNAs. The DE-mRNAs in the 122 IDH^{WT} and 10 IDH^{MT} GBM samples were also explored. Heatmap clustering revealed that IDH^{MT} GBMs exhibited distinct mRNA expression patterns compared with IDH^{WT} GBMs (Fig. 2A). A total of 142 upregulated and 219 downregulated lncRNAs were identified in IDH^{MT} GBMs (Fig. 2B). Univariate Cox model analysis of DE-mRNAs revealed 47 survival-related mRNAs, including 10 protective and 37 risk mRNAs (P<0.01; Table SIII). In addition, multivariate Cox regression analysis identified a fifteen-mRNA prognostic signature that predicted the survival of patients with GBM, including four protective mRNAs: BMP2, MSTN, ATP13A5, Histone cluster 3 H2a and 11 risk-associated mRNAs: Carboxylesterase 1 (CES1), G protein-coupled receptor 1 (GPR1), Testis expressed 261, WAP four-disulfide core domain 2 (WFDC2), Salute carrier family 16 member 11, Desmin, AHNAK nucleoprotein 2 (AHNAK2), DNA damage inducible transcript 4 like, SH3 and cysteine rich domain 2 and Pentraxin 3 (PTX3), as presented in Fig. 2C and Table II. Patients were also divided into low/high-risk groups according to the median risk score. Kaplan-Meier survival analysis revealed that the OS time of patients in the high-risk group was significantly shorter compared with the low-risk group (P<0.001; HR=3.284; 95% CI, 2.972-7.072; Fig. 2D). Therefore, the mRNA profile analysis revealed 15 prognostic mRNAs that may serve roles in determining the distinct properties of IDH^{WT} and IDH^{MT} GBMs.

Cox regression analysis was performed to determine if the prognostic capacities of the three-lncRNA and fifteen-mRNA signatures were independent of the other clinical variables in patients with GBM, including age, sex, KPS and IDH mutation status. As presented in Table III, patient IDH mutation status combined with the three-lncRNA and fifteen-mRNA signature significantly predicted the survival of patients with GBM in the univariate Cox model. In the multivariate Cox model, the three-lncRNA and the fifteen-mRNA

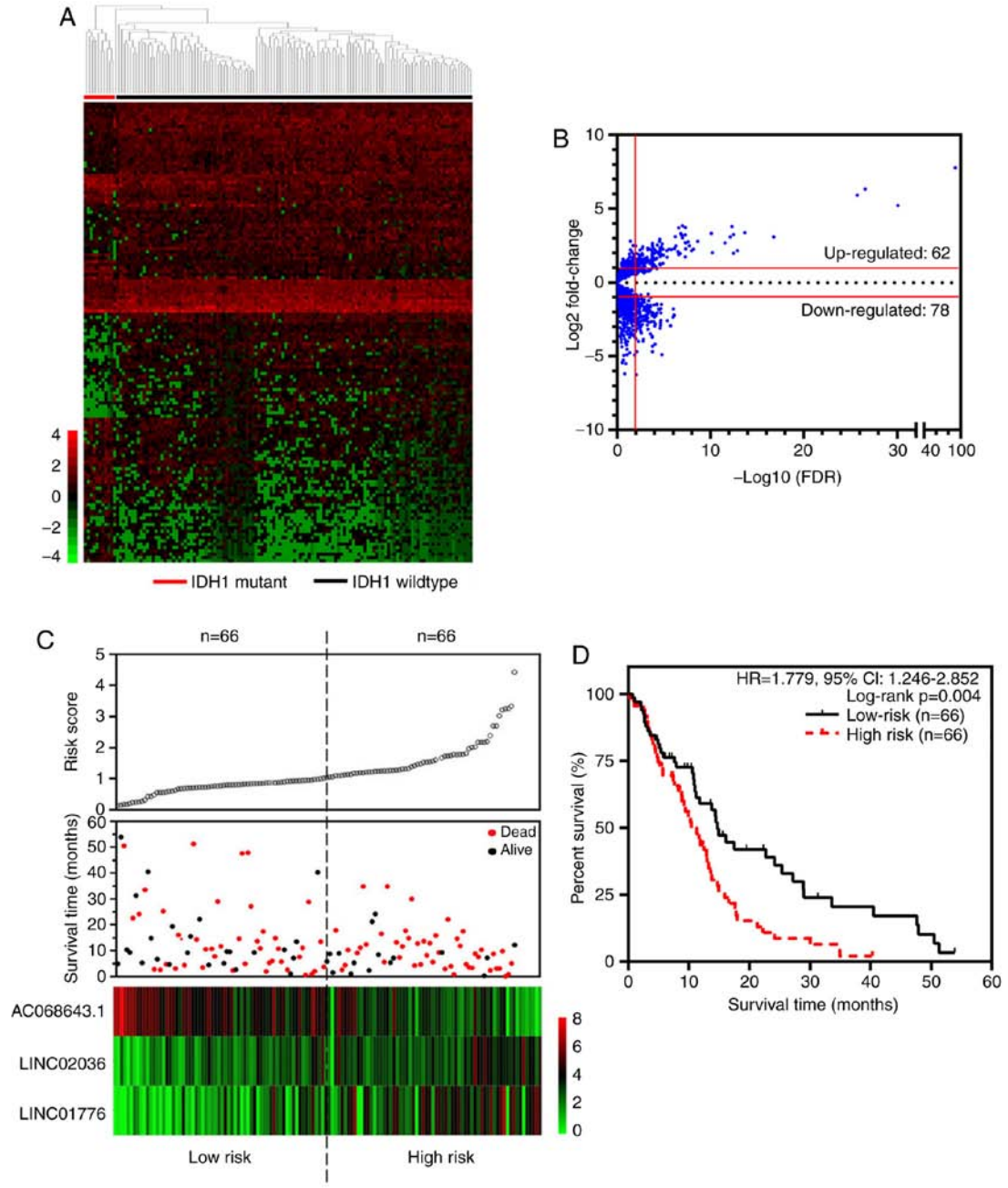

Figure 1. Identification of prognostic DE-lncRNAs in IDH^{MT} and IDH^{WT} GBMs. (A) Heatmap of DE-lncRNAs between IDH^{WT} and IDH^{MT} GBM subtypes (n=122 and n=10, respectively). Each row represents an individual lncRNA and each column represents an individual sample. (B) Volcano plot of DE-lncRNAs in IDH^{WT} and IDH^{MT} GBM subtypes (n=122 and n=10, respectively). Blue dots represent all tested lncRNAs. Red lines represent the threshold value of fold-change and adjusted P-value of DE-lncRNAs. Significant DE-lncRNAs were filtered based on $\log_2$ fold-change ≥1/≤-1 and $-\log_{10}$ adjusted P-value ≥2. (C) Three prognostic DE-lncRNAs that categorize patients with GBM into low and high-risk groups: Top, lncRNA risk score distribution; middle, patient survival; bottom, low and high score groups for the three lncRNAs (AC068643.1, Linc01776 and Linc02036). (D) Kaplan-Meier survival analysis of patients in the low and high-risk groups. DE-lncRNAs, differentially expressed long non-coding RNAs; IDH^{MT}, isocitrate dehydrogenase mutant; IDH^{WT}, isocitrate dehydrogenase wild-type; GBMs, glioblastomas; FDR, adjusted P-value; HR, hazard ratio; CI, confidence interval.

signatures remained significant prognostic markers for patients with GBM (Table III). These results suggested that the three-lncRNA and fifteen-mRNA signatures may serve roles in mediating the different behaviors observed in IDH^{MT} and IDH^{WT} GBMs and contribute to the distinct prognosis of these patients.

Association between the three-lncRNA and the fifteen-mRNA signatures. First, the correlations between the expression of the three lncRNAs and the 19,676 mRNAs from the whole genome were investigated. Pearson's correlation analysis identified 337 mRNAs co-expressed with the three lncRNAs (r>0.4), 187 of which were co-expressed with AC068643.1, 145 with Linc02036 and 5 with Linc01776 (Fig. 3A-C). Functional enrichment analyses revealed that these co-expressed mRNAs were significantly enriched in 19 GO terms and 5 KEGG pathways (P<0.05; Fig. 3D and E), which were primarily involved in regulating

Table I. Detailed information of the prognostic three-lncRNA signature from The Cancer Genome Atlas database.

Ensemble ID	lncRNA	Position	HR	P-value
ENSG00000257703	AC068643.1	Chr12:103080950-103178675: -1	0.754	0.001[a]
ENSG00000226053	LINC01776	Chr1:98210747-98272658: 1	1.234	0.001[a]
ENSG00000225742	LINC02036	Chr3:194203016-194250153: -1	1.385	0.001[a]

[a]P<0.001. lncRNA, long non-coding RNA; Chr, chromosome.

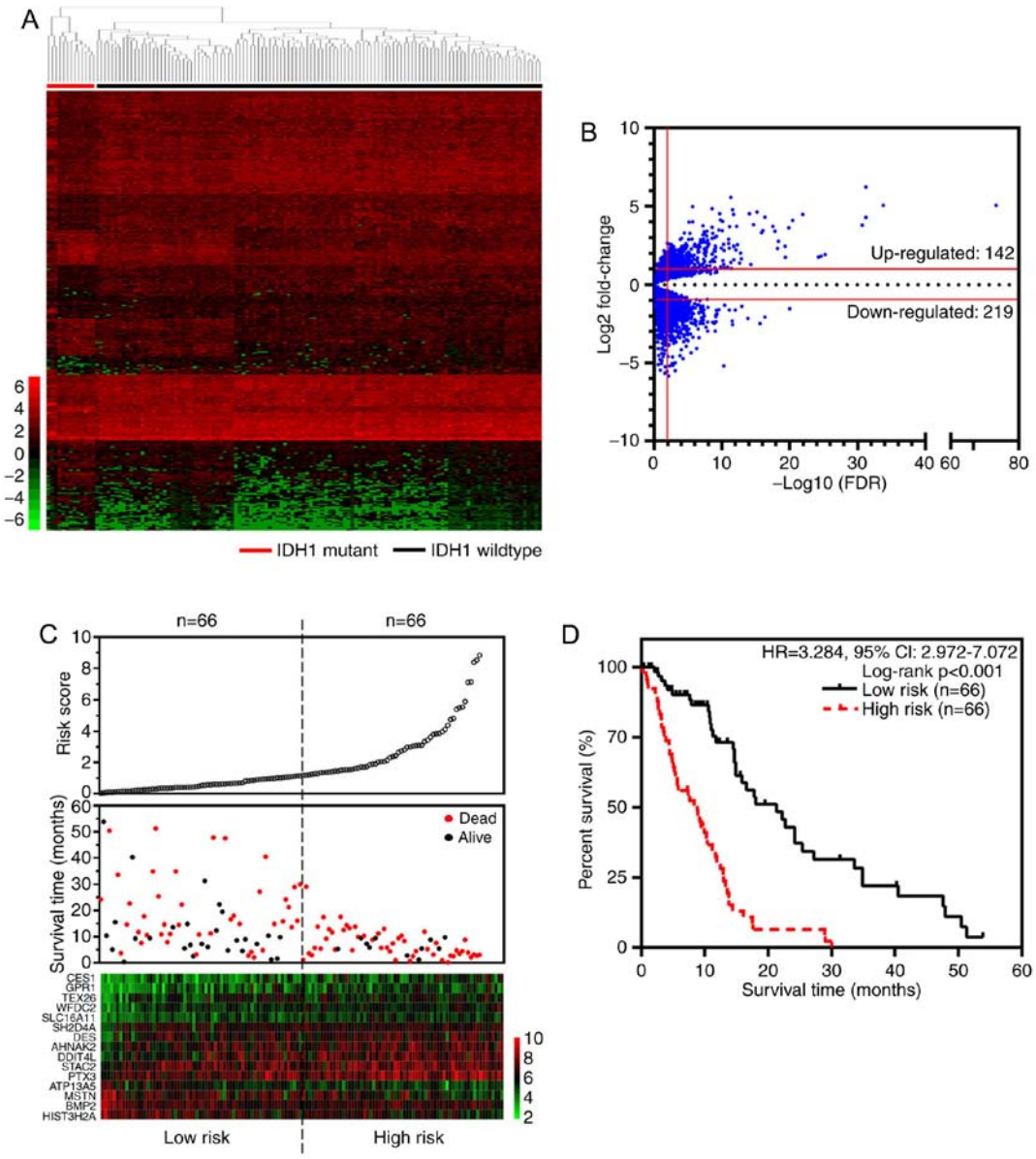

Figure 2. Identification of prognostic DE-mRNAs between IDH^{MT} and IDH^{WT} GBMs. (A) Heatmap of DE-mRNAs between IDH^{WT} and IDH^{MT} GBMs subtypes (n=122 and n=10, respectively). Each row represents an individual mRNA and each column represents an individual sample. (B) Volcano plot of DE-mRNAs in IDH^{WT} and IDH^{MT} GBMs. Blue dots represent all tested mRNAs. Red lines represent the threshold value of fold-change and adjusted P-value of DE-mRNAs. Significant DE-mRNAs were filtered based on $\log_2$ fold-change ≥1/≤-1 and $-\log_{10}$ adjusted P-value ≥2. (C) Fifteen prognostic DE-mRNAs used to classify GBM patients into low and high-risk groups: Top, mRNA risk score distribution; middle, patient survival; bottom, low and high score groups for the fifteen mRNAs. (D) Kaplan-Meier survival analysis of patients in the low- and high-risk groups. DE-mRNAs, differentially expressed mRNAs; IDH^{MT}, isocitrate dehydrogenase mutant; IDH^{WT}, isocitrate dehydrogenase wild-type; GBMs, glioblastomas; FDR; adjusted P-value; HR, hazard ratio; CI, Confidence interval.

stem cell pluripotency, Hippo and Wnt signaling pathways and cell differentiation.

The mRNAs co-expressed with the fifteen signature DE-mRNAs were analyzed; the protective DE-lncRNA

Table II. Detailed information of the prognostic fifteen-mRNA signature from The Cancer Genome Atlas database.

Ensemble IDs	mRNA	Position	HR	P-value
ENSG00000198848	CES1	Chr16:55802851-55833337: -1	1.179	0.001[b]
ENSG00000169508	GPR1	Chr13:99294530-99307405: -1	1.172	0.002[a]
ENSG00000175664	TEX261	Chr13:30932703-30975502: 1	1.198	0.005[a]
ENSG00000101443	WFDC2	Chr20:45469706-45481532: 1	1.339	0.001[b]
ENSG00000174326	SLC16A11	Chr17:7041630-7043923: -1	1.284	0.001[b]
ENSG00000175084	DES	Chr2:219418377-219426739: 1	1.152	0.009[a]
ENSG00000185567	AHNAK2	Chr14:104937244-104978357: -1	1.187	0.004[a]
ENSG00000145358	DDIT4L	Chr4:100185870-100190782: -1	1.203	0.001[b]
ENSG00000141750	STAC2	Chr17:39210536-39225872: -1	1.179	0.006[a]
ENSG00000163661	PTX3	Chr3:157436789-157443628: 1	1.244	0.001[b]
ENSG00000187527	ATP13A5	Chr3:193274790-193378843: -1	0.799	0.001[b]
ENSG00000138379	MSTN	Chr2:190055697-190062729: -1	0.857	0.002[a]
ENSG00000125845	BMP2	Chr20:6767664-6780280:1	0.769	0.006[a]
ENSG00000181218	HIST3H2A	Chr1:228456979-228457873: -1	0.839	0.001[b]

[a]P<0.01, [b]P<0.001. Chr, chromosome; HR, hazard ratio; CES1, Carboxylesterase 1; GPR1, G protein-coupled receptor 1; TEX261, Testis expressed 261; SLC16A11, Salute carrier family 16 member 11; DES, Desmin; AHNAK2, AHNAK nucleoprotein 2; DDIT4L, DNA damage inducible transcript 4 like; STAC2, SH3 and cysteine rich domain 2; PTX3, Pentraxin 3; ATP13A5, ATPase 13 A5; MSTN, Myostatin; BMP2, Bone morphogenetic protein 2; HIST3H2A, Histone cluster 3 H2a.

Table III. Univariate and Multivariate Cox Regression analyses of the prognostic three-lncRNA and fifteen-mRNA signatures.

	Univariate			Multivariate		
Variables	HR	95% CI	P-value	HR	95% CI	P-value
Sex, male vs. female	-	-	0.212	-	-	0.363
Age at diagnosis, years, ≥40 vs. <40	-	-	0.098	-	-	0.304
Karnofsky performance status, ≤70 vs. >70	-	-	0.331	-	-	0.33
IDH status, mutant vs. wild-type	0.271	0.108-0.683	0.006[a]	-	-	0.076
lncRNA signature, high vs. low	2.771	1.772-4.332	0.001[b]	2.701	1.642-4.443	0.001[b]
mRNA signature, high vs. low	4.094	2.571-6.521	0.001[b]	4.624	2.744-7.792	0.001[b]

[a]P<0.01, [b]P<0.001. HR, hazard ratio; CI, confidence interval; lncRNA, long non-coding RNA; IDH, isocitrate dehydrogenase; High, high risk score; Low, low risk score.

AC068643.1 was significantly correlated with three protective signature mRNAs: BMP2 (r=0.403; P<0.001), MSTN (r=0.415; P<0.001) and ATP13A5 (r=0.471; P<0.001) as presented in Figs. 3A and S1A-C. BMP2 and MSTN both belong to the BMP-signaling pathway (27), thus it was predicted that AC068643.1 may function through interaction with the BMP signaling pathway. qPCR analysis of GBM samples from the XQ cohort demonstrated that protective lncRNA AC068643.1, BMP2 and MSTN were upregulated in IDH^{MT} GBMs (Fig. 4A-C), and AC068643.1 was significantly positively correlated with BMP2 (r=0.427; P=0.004) and MSTN (r=0.395; P=0.010; Fig. 4D and E). RNA profiling data from the CGGA database confirmed that BMP2 and MSTN expression levels were upregulated in IDH^{MT} compared with IDH^{WT} GBMs, predicting a favorable prognosis for these patients (Fig. S1D-G). These results indicated an association between AC068643.1, BMP2 and MSTN.

Following treatment with BMP2 and MSTN cytokines in cell culture medium, AC068643.1 expression levels were significantly upregulated in T98G cells treated with different concentrations (0, 10 and 50 ng/ml) of BMP2 or MSTN (Fig. 4F). These results suggested that upregulated BMP signaling may promote IDH^{MT} GBM differentiation through promoting AC068643.1 expression.

Functional analysis of lncRNA AC068643.1. To investigate the function of AC068643.1, GO and KEGG analysis of the 187 co-expressed mRNAs of AC068643.1 were performed. The results suggested that AC068643.1 was associated with 'mitochondrial matrix', 'regulation of transcription, DNA-templated',

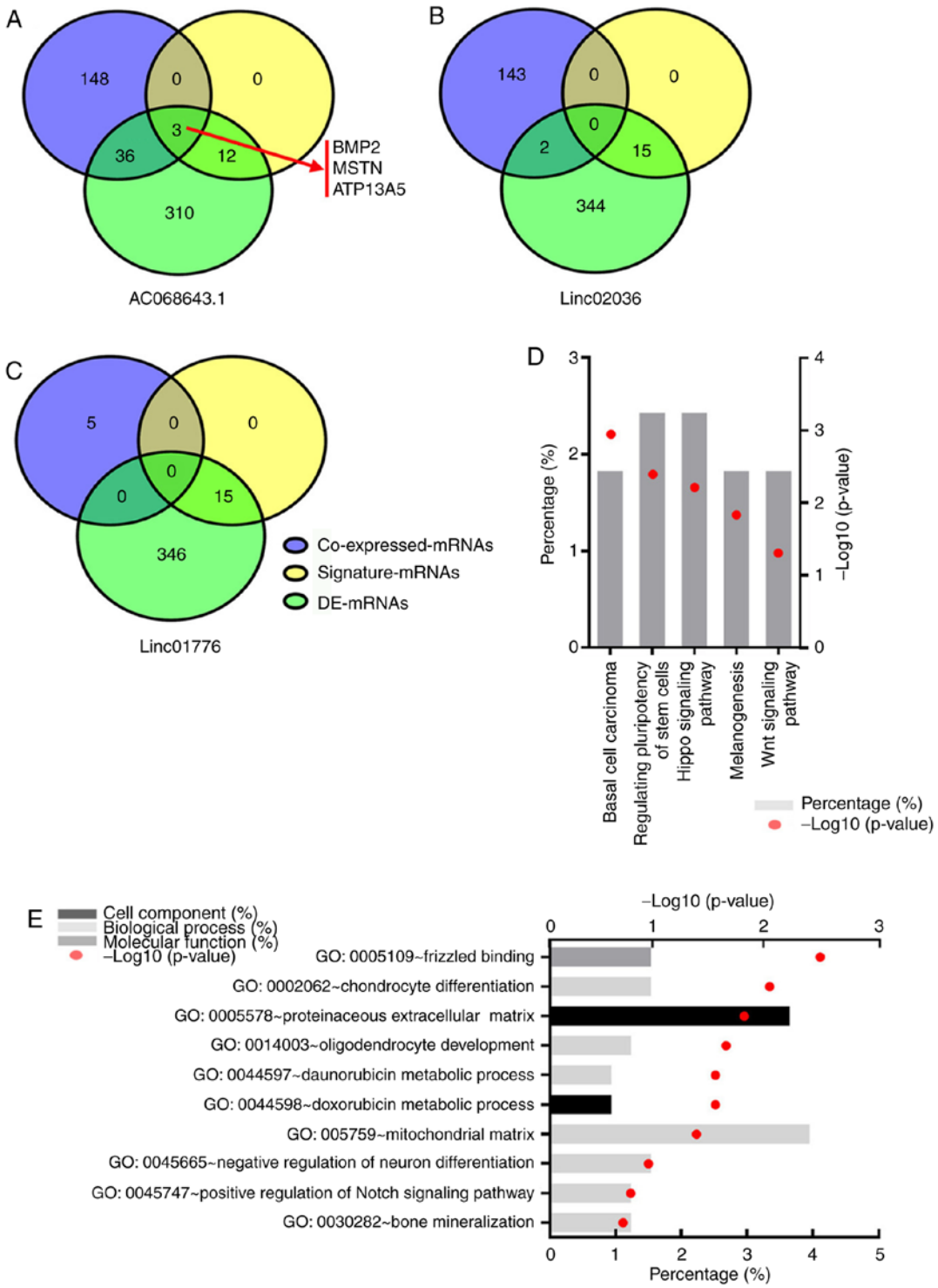

Figure 3. Functional assessment of the three-lncRNA signature (AC068643.1, Linc01776 and Linc02036). (A-C) Venn diagram analysis showing the interaction of co-expressed mRNAs, signature mRNAs and DE-mRNAs for each signature lncRNA: (A) AC068643.1, (B) Linc01776 and (C) Linc02036. (D) Kyoto Encyclopedia of Genes and Genomes and (E) Gene Ontology gene enrichment analyses of mRNAs co-expressed with the three signature lncRNAs. lncRNA, long non-coding mRNA; DE-mRNAs, differentially expressed mRNAs; GO, Gene Ontology.

'nucleic acid binding' and 'regulation of pluripotency of stem cells' (Fig. S2A and B). In addition, subcellular expression of AC068643.1 was detected using different glioma cell lines, including SF295, SF268, LN229 and T98G, and the results demonstrated that AC068643.1 exhibited low expression levels and was primarily expressed in the glioma cell nucleus (Fig. 4G), which was consistent with the gene enrichment analysis.

Discussion

The discovery of IDH mutations changed the classification system of glioma, leading to the acknowledgement of the IDH^{WT} and IDH^{MT} subtypes (6). Studies investigating the role of IDH mutations in IDH^{MT} gliomas have aimed to treat this glioma subtype through IDH mutation-targeted treatment (28,29),

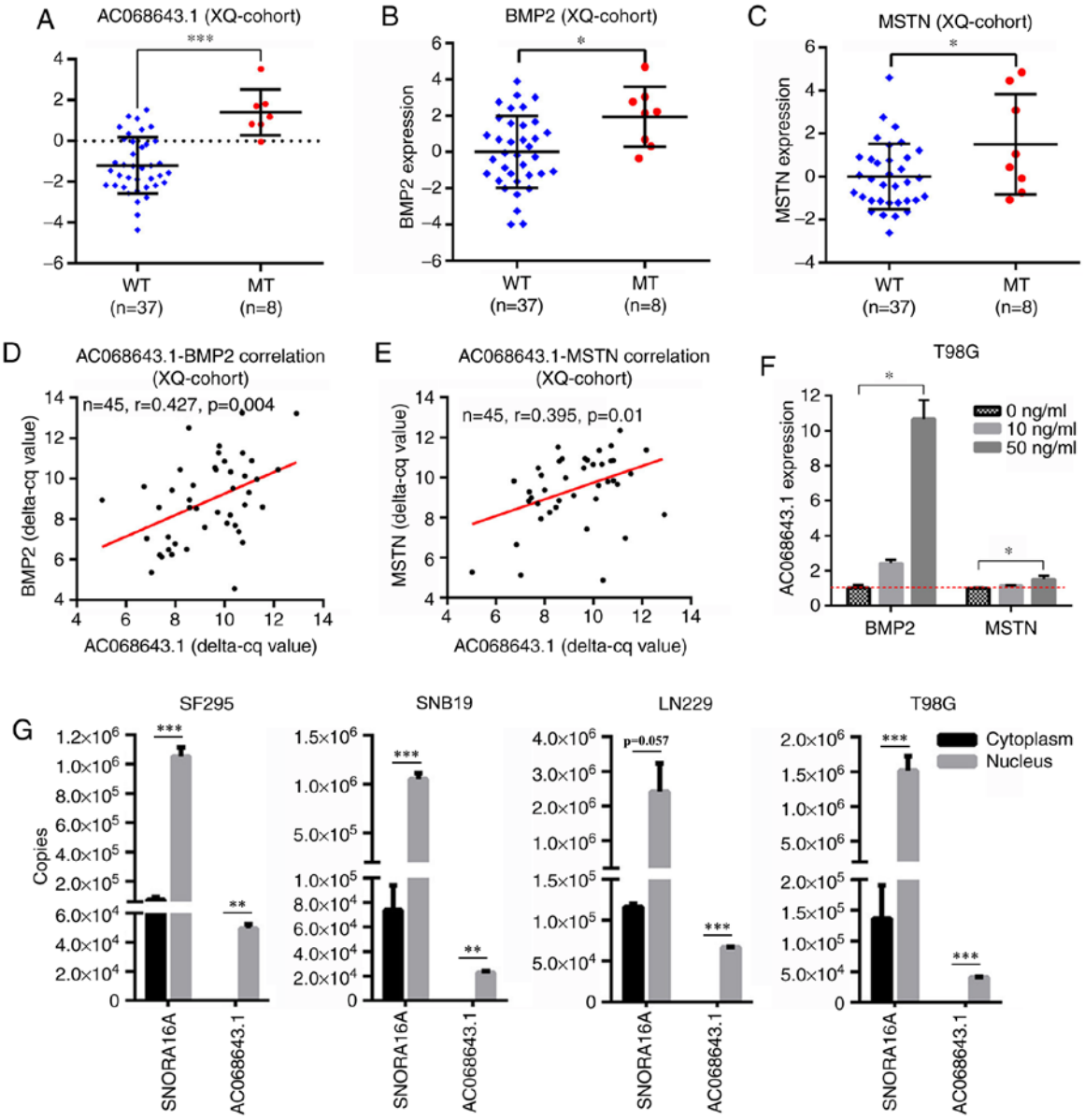

Figure 4. Functional analysis of AC068643.1. (A) qPCR analysis demonstrated that lncRNA AC068643.1 expression levels were upregulated in *IDH*^{MT} compared with *IDH*^{WT} GBMs. (B and C) qPCR detection showed that (B) BMP2 and (C) MSTN expression levels were upregulated in *IDH*^{MT} compared with *IDH*^{WT} GBMs. (D and E) Pearson correlation analyses revealed that AC068643.1 was significantly positively correlated with (D) BMP2 and (E) MSTN in GBMs samples from the XQ cohort. (F) qPCR analysis revealed that AC068643.1 expression levels were upregulated by BMP2 and MSTN treatment. (G) Subcellular qPCR detection of lncRNA AC068643.1 in SF295, SNB19, LN229 and T98G glioma cell lines demonstrated that AC068643.1 was primarily expressed in the nucleus and at low levels. *P<0.05, **P<0.01 and ***P<0.001. qPCR, quantitative PCR; lncRNA, long non-coding mRNA; *IDH*^{MT}, isocitrate dehydrogenase mutant; *IDH*^{WT}, isocitrate dehydrogenase wild-type; GBMs, glioblastomas; XQ, Xinqiao Hospital; BMP2, Bone morphogenetic protein 2; MSTN, Myostatin.

whereas the mechanisms underlying *IDH*^{WT} glioma, which exhibits a higher degree of malignancy and accounts for >70% of all GBMs (5), have been somewhat neglected. The present study aimed to explore the altered lncRNA/mRNAs expression levels between *IDH*^{WT} and *IDH*^{MT} gliomas, the results of which may provide insight into understanding the biological behaviors of *IDH*^{WT} GBM.

The present study utilized comprehensive Agilent RNA-profiling data containing ~10,000 lncRNAs in each sample. *IDH*^{MT} GBMs only constitute a small proportion of GBMs cases (~5.6%) (5), and thus data for only 10 *IDH*^{MT} GBM cases were obtained from TCGA, compared with 122 cases of IDH^{WT} GBM, which is a limitation of the present study. A total of 140 DE-lncRNAs and 361 DE-mRNAs between *IDH*^{WT} and *IDH*^{MT} GBMs were identified. Three-lncRNA and fifteen-mRNA signatures with prognostic value were identified, suggesting that these lncRNAs and mRNAs may function in determining the distinct properties between *IDH*^{WT} and *IDH*^{MT} GBMs. Gene enrichment analysis revealed that the three-lncRNA signature was associated with cell differentiation-associated KEGG pathways and GO terms. By contrast, seven mRNAs from the fifteen-mRNA signature, including: five risk mRNAs, CES1 (30), GPR1 (31), WFDC2 (32), AHNAK2 (33) and PTX3 (34), and two protective mRNAs, BMP2 (35) and MSTN (36), were associated with cell stemness or cell differentiation. These results suggested that cell differentiation/stemness status may be the primary distinct property between *IDH*^{WT} and *IDH*^{MT} GBMs.

Previous studies have demonstrated that tumor stem cells are responsible for tumor growth, chemoresistance and relapse, and that tumor stemness is associated with poor patient survival outcomes (37,38). The results of the present study indicated that the distinct tumor behaviors and clinical features between IDH^{WT} and IDH^{MT} GBMs may be partially due to the different cell differentiation status. A recent study has reported that the stem cell markers nestin and CD133 are significantly upregulated in IDH^{WT} compared with IDH^{MT} gliomas (39). Overexpression of IDH mutant protein in glioma stem cells downregulates nestin and CD133 expression levels and promotes glioma stem cell differentiation via the Wnt/β-catenin pathway (39), providing further evidence that varied differentiation/stemness status between IDH^{WT} and IDH^{MT} GBMs may be a contributing factor for their distinct behaviors.

BMP2 and MSTN belong to the BMP signaling pathway, which can prevent cell self-renewal and enhance differentiation (27). In the present study, the expression levels of AC068643.1 were significantly positively correlated with those of BMP2 and MSTN, suggesting that there may be a potential positive regulatory axis between AC068643.1 and the BMP signaling pathway responsible for promoting glioma differentiation. *In vitro* treatment of T98G cells with BMP2 and MSTN significantly upregulated AC068643.1 expression, suggesting that AC068643.1 expression level is regulated by the BMP signaling pathway. Future studies should focus on exploring the effects of AC068643.1 knockdown or overexpression in the BMP signaling pathway and glioma differentiation.

In conclusion, by comparing the transcriptome profiling data between IDH^{MT} and IDH^{WT} GBMs, the present study identified stemness-related three-lncRNA and fifteen-mRNA signatures, suggesting that cell differentiation or stemness status may be a primary property which is distinct between IDH^{WT} and IDH^{MT} GBMs. Protective lncRNA AC068643.1 was significantly upregulated in IDH^{MT} GBMs and was positively regulated by BMP2 and MSTN, which suggested that AC068643.1 overexpression may prevent glioma self-renewal and enhance cell differentiation. These results may aid our understanding of the more differentiated status and the more favorable prognosis of IDH^{MT} compared with IDH^{WT} GBMs and may provide a basis for IDH^{WT} GBM treatment by inducing lncRNA AC068643.1 overexpression.

Acknowledgements

The authors would like to thank Miss. Qing-Rui Li (Department of Pathology Southwest Hospital, Third Military Medical University) for her work in collecting clinical samples and patients' follow-up and Professor Shuli Xia (Department of Neurology, Johns Hopkins School of Medicine) for her supervison and revision of this study.

Funding

The present study was supported by the National Natural Science Foundation of China (grant no. NSFC:81972360).

Availability of data and materials

The datasets used and/or analyzed during the present study are available from the corresponding author on reasonable request.

Authors' contributions

GHH, SQL and JL conceived and designed the experiments. GHH, YCP, LY, KJM and YX performed the experiments and data statistics. GHH and JHT discussed and interpreted the data. GHH wrote the manuscript. SQL supervised the study. All authors read and approved the final manuscript.

Ethics approval and consent to participate

The present study was approved by The Medical Ethics Committee of the Second Affiliated Hospital of the Third Military Medical University.

Patient consent for publication

Not applicable.

Competing interests

The authors declare that they have no competing interests.

References

1. Louis DN, Perry A, Reifenberger G, von Deimling A, Figarella-Branger D, Cavenee WK, Ohgaki H, Wiestler OD, Kleihues P and Ellison DW: The 2016 World Health organization classification of tumors of the central nervous system: A summary. Acta Neuropathol 131: 803-820, 2016.
2. Stupp R, Mason WP, van den Bent MJ, Weller M, Fisher B, Taphoorn MJ, Belanger K, Brandes AA, Marosi C, Bogdahn U, *et al*: Radiotherapy plus concomitant and adjuvant temozolomide for glioblastoma. N Engl J Med 352: 987-996, 2005.
3. Gilbert MR, Dignam JJ, Armstrong TS, Wefel JS, Blumenthal DT, Vogelbaum MA, Colman H, Chakravarti A, Pugh S, Won M, *et al*: A randomized trial of bevacizumab for newly diagnosed glioblastoma. N Engl J Med 370: 699-708, 2014.
4. Vredenburgh JJ, Desjardins A, Herndon JE II, Dowell JM, Reardon DA, Quinn JA, Rich JN, Sathornsumetee S, Gururangan S, Wagner M, *et al*: Phase II trial of bevacizumab and irinotecan in recurrent malignant glioma. Clin Cancer Res 13: 1253-1259, 2007.
5. Yan H, Parsons DW, Jin G, McLendon R, Rasheed BA, Yuan W, Kos I, Batinic-Haberle I, Jones S, Riggins GJ, *et al*: IDH1 and IDH2 mutations in gliomas. N Engl J Med 360: 765-773, 2009.
6. Turkalp Z, Karamchandani J and Das S: IDH mutation in glioma: New insights and promises for the future. JAMA Neurol 71: 1319-1325, 2014.
7. Wang RA: MTA1-a stress response protein: A master regulator of gene expression and cancer cell behavior. Cancer Metastasis Rev 33: 1001-1009, 2014.
8. Wang KC and Chang HY: Molecular mechanisms of long noncoding RNAs. Mol Cell 43: 904-914, 2011.
9. Carninci P, Kasukawa T, Katayama S, Gough J, Frith MC, Maeda N, Oyama R, Ravasi T, Lenhard B, Wells C, *et al*: The transcriptional landscape of the mammalian genome. Science 309: 1559-1563, 2005.
10. Mercer TR, Dinger ME, Sunkin SM, Mehler MF and Mattick JS: Specific expression of long noncoding RNAs in the mouse brain. Proc Natl Acad Sci USA 105: 716-721, 2008.
11. Qureshi IA, Mattick JS and Mehler MF: Long non-coding RNAs in nervous system function and disease. Brain Res 1338: 20-35, 2010.
12. Cuevas-Diaz Duran R, Wei H, Kim DH and Wu JQ: Invited Review: Long non-coding RNAs: Important regulators in the development, function and disorders of the central nervous system. Neuropathol Appl Neurobiol 45: 538-556, 2019.
13. Zhang XQ and Leung GK: Long non-coding RNAs in glioma: Functional roles and clinical perspectives. Neurochem Int 77: 78-85, 2014.

14. Ramos AD, Attenello FJ and Lim DA: Uncovering the roles of long noncoding RNAs in neural development and glioma progression. Neurosci Lett 625: 70-79, 2016.
15. Han L, Zhang K, Shi Z, Zhang J, Zhu J, Zhu S, Zhang A, Jia Z, Wang G, Yu S, *et al*: LncRNA profile of glioblastoma reveals the potential role of lncRNAs in contributing to glioblastoma pathogenesis. Int J Oncol 40: 2004-2012, 2012.
16. Chen Q, Cai J, Wang Q, Wang Y, Liu M, Yang J, Zhou J, Kang C, Li M and Jiang C: Long Noncoding RNA NEAT1, Regulated by the EGFR pathway, contributes to glioblastoma progression through the WNT/β-catenin pathway by scaffolding EZH2. Clin Cancer Res 24: 684-695, 2018.
17. Pastori C, Kapranov P, Penas C, Peschansky V, Volmar CH, Sarkaria JN, Bregy A, Komotar R, St Laurent G, Ayad NG, *et al*: The Bromodomain protein BRD4 controls HOTAIR, a long noncoding RNA essential for glioblastoma proliferation. Proc Natl Acad Sci USA 112: 8326-8331, 2015.
18. Zhang JX, Han L, Bao ZS, Wang YY, Chen LY, Yan W, Yu SZ, Pu PY, Liu N, You YP, *et al*: HOTAIR, a cell cycle-associated long noncoding RNA and a strong predictor of survival, is preferentially expressed in classical and mesenchymal glioma. Neuro Oncol 15: 1595-1603, 2013.
19. Mineo M, Ricklefs F, Rooj AK, Lyons SM, Ivanov P, Ansari KI, Nakano I, Chiocca EA, Godlewski J and Bronisz A: The Long Non-coding RNA HIF1A-AS2 facilitates the maintenance of mesenchymal glioblastoma stem-like cells in hypoxic niches. Cell Rep 15: 2500-2509, 2016.
20. Rutka JT, Giblin JR, Dougherty DY, Liu HC, McCulloch JR, Bell CW, Stern RS, Wilson CB and Rosenblum ML: Establishment and characterization of five cell lines derived from human malignant gliomas. Acta Neuropathol 75: 92-103, 1987.
21. Tang JH, Ma ZX, Huang GH, Xu QF, Xiang Y, Li N, Sidlauskas K, Zhang EE and Lv SQ: Downregulation of HIF-1a sensitizes U251 glioma cells to the temozolomide (TMZ) treatment. Exp Cell Res 343: 148-158, 2016.
22. Livak KJ and Schmittgen TD: Analysis of relative gene expression data using real-time quantitative PCR and the 2(-Delta Delta C(T)) method. Methods 25: 402-408, 2001.
23. Zhu Y, Qiu P and Ji Y: TCGA-assembler: Open-source software for retrieving and processing TCGA data. Nat Methods 11: 599-600, 2014.
24. R Core Team. R: A language and environment for statistical computing. R Foundation for Statistical Computing Vienna, Austria. 2012 ISBN 3-900051-07-0, URL http://www.R-project.org/.
25. RStudio Team. RStudio: Integrated Development for R. RStudio, Inc., Boston, MA 2015. URL http://www.rstudio.com/.
26. Zhang Y, He W and Zhang S: Seeking for correlative genes and signaling pathways with bone metastasis from breast cancer by integrated analysis. Front Oncol 9: 138, 2019.
27. Caja L, Bellomo C and Moustakas A: Transforming growth factor beta and bone morphogenetic protein actions in brain tumors. FEBS Lett 589: 1588-1597, 2015.
28. Rohle D, Popovici-Muller J, Palaskas N, Turcan S, Grommes C, Campos C, Tsoi J, Clark O, Oldrini B, Komisopoulou E, *et al*: An inhibitor of mutant IDH1 delays growth and promotes differentiation of glioma cells. Science 340: 626-630, 2013.
29. Pusch S, Krausert S, Fischer V, Balss J, Ott M, Schrimpf D, Capper D, Sahm F, Eisel J, Beck AC, *et al*: Pan-mutant IDH1 inhibitor BAY 1436032 for effective treatment of IDH1 mutant astrocytoma in vivo. Acta Neuropathol 133: 629-644, 2017.
30. Seno A, Kasai T, Ikeda M, Vaidyanath A, Masuda J, Mizutani A, Murakami H, Ishikawa T and Seno M: Characterization of gene expression patterns among artificially developed cancer stem cells using spherical self-organizing map. Cancer Inform 15: 163-178, 2016.
31. Tummler C, Snapkov I, Wickstrom M, Moens U, Ljungblad L, Maria Elfman LH, Winberg JO, Kogner P, Johnsen JI and Sveinbjørnsson B: Inhibition of chemerin/CMKLR1 axis in neuroblastoma cells reduces clonogenicity and cell viability in vitro and impairs tumor growth in vivo. Oncotarget 8: 95135-95151, 2017.
32. Hofman VJ, Moreilhon C, Brest PD, Lassalle S, Le Brigand K, Sicard D, Raymond J, Lamarque D, Hébuterne XA, Mari B, *et al*: Gene expression profiling in human gastric mucosa infected with Helicobacter pylori. Mod Pathol 20: 974-989, 2007.
33. Wang M, Li X, Zhang J, Yang Q, Chen W, Jin W, Huang YR, Yang R and Gao WQ: AHNAK2 is a novel prognostic marker and oncogenic protein for clear cell renal cell carcinoma. Theranostics 7: 1100-1113, 2017.
34. Thomas C, Henry W, Cuiffo BG, Collmann AY, Marangoni E, Benhamo V, Bhasin MK, Fan C, Fuhrmann L, Baldwin AS, *et al*: Pentraxin-3 is a PI3K signaling target that promotes stem cell-like traits in basal-like breast cancers. Sci Signal 10: pii: eaah4674, 2017.
35. Persano L, Pistollato F, Rampazzo E, Della Puppa A, Abbadi S, Frasson C, Volpin F, Indraccolo S, Scienza R and Basso G: BMP2 sensitizes glioblastoma stem-like cells to Temozolomide by affecting HIF-1α stability and MGMT expression. Cell Death Dis 3: e412, 2012.
36. Di Fiore R, Fanale D, Drago-Ferrante R, Chiaradonna F, Giuliano M, De Blasio A, Amodeo V, Corsini LR, Bazan V, Tesoriere G and Vento R: Genetic and molecular characterization of the human osteosarcoma 3AB-OS cancer stem cell line: A possible model for studying osteosarcoma origin and stemness. J Cell Physiol 228: 1189-1201, 2013.
37. Esparza R, Azad TD, Feroze AH, Mitra SS and Cheshier SH: Glioblastoma stem cells and stem cell-targeting immunotherapies. J Neurooncol 123: 449-457, 2015.
38. Sen Z, Zhan XK, Jing J, Yi Z and Wanqi Z: Chemosensitizing activities of cyclotides from Clitoria ternatea in paclitaxel-resistant lung cancer cells. Oncol Lett 5: 641-644, 2013.
39. Yao Q, Cai G, Yu Q, Shen J, Gu Z, Chen J, Shi W and Shi J: IDH1 mutation diminishes aggressive phenotype in glioma stem cells. Int J Oncol 52: 270-278, 2018.